J. Membrane Biol. 42, 215–227 (1978)

Comparison of Ion Current Noise Predicted from Different Models of the Sodium Channel Gating Mechanism in Nerve Membrane

John R. Clay

Department of Anatomy, Emory University, Atlanta, Georgia 30322

Received 31 January 1978

Summary. The theoretical power density spectrum $S(f)$ of ion current noise is calculated from several models of the sodium channel gating mechanism in nerve membrane. Sodium ion noise experimental data from the frog node of Ranvier [Conti, F., *et al.* (1976), *J. Physiol. (London)* **262**:699] is used as a test of the theoretical results. The motivation for recent modeling has been evidence for a coupling between sodium activation and inactivation from voltage clamp data. The two processes are independent of one another in the Hodgkin and Huxley (HH) model [Hodgkin, A.L., Huxley, A.F. (1952), *J. Physiol. (London)* **117**:500]. The noise data is consistent with HH, as noted by Conti *et al.* (1976). The theoretical results given here appear to indicate that only one case of coupling models is also consistent with the noise data.

Recent voltage clamp experiments on nerve axons have indicated that the Hodgkin and Huxley (1952) model of sodium conductance of axonal membrane is not entirely adequate (*cf.* Jakobsson, 1978). For example, the time constant for deconditioning the Na current during a depolarizing clamp step is slower than the time constant for turning off the current during the same step. This phenomenon has been observed in giant axons of *Myxicola* (Goldman & Schauf, 1973) and lobster (Oxford & Pooler, 1975), and in some axons of the blue crab walking leg (Connor, 1976); however, other crab axons do not show it (Connor, 1976), nor does the frog node of Ranvier (Chiu, 1976). The HH model predicts that these two time constants should be the same. A second difference is a delay in the onset of inactivation in response to a depolarizing pulse which is preceded by a conditioning pulse of variable duration. That is, the dependence of inactivation on the duration of the conditioning pulse is sigmoidal rather than exponential, as predicted by HH. *Myxicola* axons

0022-2631/78/0042-0215 $02.60

(Goldman & Schauf, 1973), frog node of Ranvier (Peganov, 1973) and giant axons from squid (Bezanilla & Armstrong, 1977) exhibit the effect. Thirdly, measurements of gating currents from squid axons (Armstrong & Bezanilla, 1977) indicate that several time constants are required to describe the Na ion gating mechanism. The HH model provides only two.

These observations suggest that the inactivation process is coupled in some way to the activation of Na ion current. The two processes are independent of one another in the HH model. A few alternative models have been proposed recently to describe one or more of the above phenomena, or other deficiencies of HH (Moore & Cox, 1976; Jakobsson, 1978; Armstrong & Bezanilla, 1977). A feature common to all of them is that activation and inactivation are coupled.

The purpose of the present study is to calculate the current noise power density spectrum $S(f)$, $f \equiv$ frequency, predicted by these and related models, as well as HH, and to compare the theoretical spectra with noise data. The results from frog node (Conti *et al.*, 1976) will be used throughout as a baseline for comparison, because their study is, perhaps, the most detailed experimental determination of $S(f)$ for the Na system to date. Unfortunately, the inadequacies of HH vary considerably from one preparation to another. Moreover, the above models have been designed primarily for squid axon, so that the comparisons made in this paper to frog node data are not completely appropriate. Nevertheless, this exercise does demonstrate that the shape of $S(f)$ is rather sensitive to the specific type of coupling proposed.

HH Model Spectrum

The calculation of $S(f)$ from a mathematical model of conductance based on macroscopic voltage clamp data is a straightforward and well documented procedure, especially for the HH equations (Hill & Chen, 1972; Stevens, 1972). One important assumption is required before this theoretical connection can be made; namely, a microscopic interpretation of the physical process underlying the macroscopic conductance variables. For example, the HH description of the time and voltage dependence of Na conductance is given by $m^3 h$, where m and h are the activation and inactivation variables, respectively. They are the solutions to the first order differential equations

$$\begin{aligned} dm/dt \equiv \dot{m} &= -(\alpha_m + \beta_m)m + \alpha_m m \\ \dot{h} &= -(\alpha_h + \beta_h)h + \alpha_h h \end{aligned} \tag{1}$$

where the α's and β's are voltage dependent parameters which are independent of time. This model has two physical interpretations (Stevens, 1972). In one, m and h specify the rotational state of two different gating molecules with m or $h=1$ referring to the particles being fully open, m or $h=0$ referring to them being fully closed, and intermediate values of the variables referring to them being fractionally open. In the second interpretation, the gating mechanism is viewed as consisting of four particles or molecular subunits, each of which is either in a fully open or fully closed position. The quantity m specifies the probability that any of the three activation particles is open and h specifies the probability that the inactivation particle is open. These two pictures give slightly different half power frequencies, so that noise data can, in principle, distinguish between them. The spectra of Conti *et al.* (1976) appear to be consistent with the discrete open-close picture. It also is supported by recent observations of discrete step-like changes in membrane current from single channels in artificial bilayers containing various macromolecules (reviewed by Neher & Stevens, 1977), and from single channels in post-synaptic muscle membrane (Neher & Sakmann, 1976). However, similar direct measurements of channel openings have not yet been reported in nerve.

In any case, the discrete open-close picture will be used in this paper because it has the further advantage of allowing a comparison of the models discussed in this paper in terms of kinetic diagrams. For example, the HH model in terms of the open-close particles,

$$\bar{m} \underset{\beta_m}{\overset{\alpha_m}{\rightleftharpoons}} m \qquad \bar{h} \underset{\beta_h}{\overset{\alpha_h}{\rightleftharpoons}} h \tag{2}$$

is equivalent to (Fitzhugh, 1965):

$$\begin{tikzcd}
{[0']} \arrow[r, shift left, "3\alpha_m"] \arrow[d, shift right, "\alpha_h"'] & {[1']} \arrow[l, shift left, "\beta_m"] \arrow[r, shift left, "2\alpha_m"] \arrow[d, shift right, "\alpha_h"'] & {[2']} \arrow[l, shift left, "2\beta_m"] \arrow[r, shift left, "\alpha_m"] \arrow[d, shift right, "\alpha_h"'] & {[3']} \arrow[l, shift left, "3\beta_m"] \arrow[d, shift right, "\alpha_h"'] \\
{[0]} \arrow[r, shift left, "3\alpha_m"] \arrow[u, shift right, "\beta_h"'] & {[1]} \arrow[l, shift left, "\beta_m"] \arrow[r, shift left, "2\alpha_m"] \arrow[u, shift right, "\beta_h"'] & {[2]} \arrow[l, shift left, "2\beta_m"] \arrow[r, shift left, "\alpha_m"] \arrow[u, shift right, "\beta_h"'] & {[3]} \arrow[l, shift left, "3\beta_m"] \arrow[u, shift right, "\beta_h"']
\end{tikzcd}$$

Diagram A

with conduction occurring only in state [3]. This diagram is simply another way of expressing the fact that the $3m$ particles and the h particle are statistically independent of one another. For example, when all 4 particles are closed, the channel is in state [0]. The probability that any single m particle opens in time Δt is $\alpha_m \Delta t$. Since any one of the three particles can open, the total probability that the channel makes a transition from [0] to [1] is $3\alpha_m \Delta t$. The other transition rates in the diagram follow from similar arguments.

Any permutation of the $3\alpha_m$, $2\alpha_m$, α_m sequence, such as the α_m, $2\alpha_m$, $3\alpha_m$ sequence proposed by Bezanilla and Armstrong (1975) and Moore and Cox (1976) necessarily implies a very different physical mechanism for the gate which cannot be described in terms of three statistically independent, open-close particles. Similarly, any modification of the way in which α_h and β_h enter into Diagram A necessarily implies a coupling between activation and inactivation. The two processes are uncoupled in A, since the rate constant from the lower to the upper (inactivated) tier of states, or vice-versa, is independent of the number of open m particles.

The single channel noise correlation function $C(t)$ for this or any other model in which conduction occurs for only one state of the kinetic diagram is given by the simple prescription (Hill & Chen, 1972; Stevens, 1972)

$$C(t)=\gamma^2(V-E)^2 P_\infty(P_0(t)-P_\infty) \tag{3}$$

where γ is the single channel conductance, E and V are the equilibrium and membrane potentials, respectively, P_∞ is the steady-state probability that the system is in the open state, and $P_0(t)$ is the probability that it is open at time t given that it was open with unit probability at $t=0$. For the HH model $P_\infty=m_\infty^3 h_\infty$, with

$$m_\infty=\alpha_m/(\alpha_m+\beta_m); \quad h_\infty=\alpha_h/(\alpha_h+\beta_h), \tag{4}$$

and

$$P_0(t)=m^3(t)h(t)|_{m(0),\,h(0)=1}=(m_\infty+(1-m_\infty)\,e^{-t/\tau_m})^3\,(h_\infty+(1-h_\infty)\,e^{-t/\tau_h}) \tag{5}$$

where

$$\tau_m=(\alpha_m+\beta_m)^{-1} \quad \text{and} \quad \tau_h=(\alpha_h+\beta_h)^{-1}. \tag{6}$$

The power density spectrum $S(f)$ is given by the Fourier transform of Eq. (3) (Wang & Uhlenbeck, 1954). That is,

$$\begin{aligned} S(f)=4\gamma^2(V-E)^2 \Big\{&((1-h_\infty)/h_\infty)L(\tau_h,f) \\ &+\sum_1^3 \binom{3}{j}((1-m_\infty)/m_\infty)^j[L(\tau_m/j,f)+((1-h_\infty)/h_\infty)L(\tau_{mjh},f)]\Big\} \end{aligned} \tag{7}$$

where $\binom{x}{y}=x!/(y!(x-y)!)$, $L(\tau,f)$ is a Lorentzian function of the form $\tau/(1+(2\pi\tau f)^2)$, and τ_{mjh} refers to $\tau_m\tau_h/(\tau_m+j\tau_h)$. This expression has also been given explicity by Conti, DeFelice, and Wanke (1975) and Conti

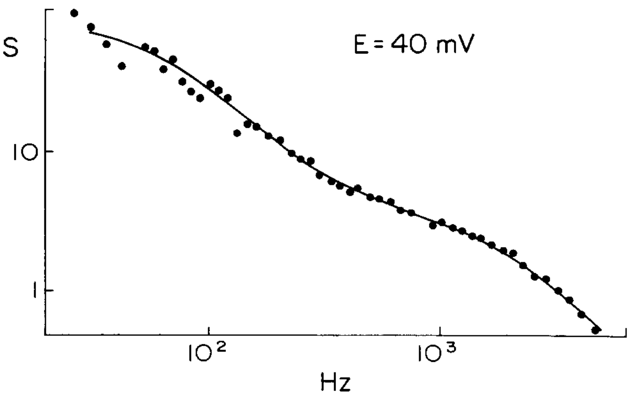

Fig. 1. Current noise power density spectrum $S(f)$ *vs.* frequency. The data points are taken from Conti *et al.* (1976) and the solid line is the theoretical $S(f)$ calculated from the HH equations, as described in the text with α's and β's appropriate for frog node of Ranvier

et al. (1976). If the individual channels are statistically independent, the total spectral density is given by the product of Eq. (7) and the number of channels N in the membrane area from which noise is measured. That is, the frequency dependence of Eq. (7) is determined by the τ's, m_∞, and h_∞, and the relative amplitude of $S(f)$ is given by $N\gamma^2$. The data from Conti *et al.* (1976) at 40 mV depolarization and the best fit of Eq. (7) which these authors obtained by varying $N\gamma^2$ are given in Fig. 1. The expressions for the α's and β's used for this comparison and for the other models examined in this study are given by Eqs. (3)–(6) of their paper. The data at 40 mV is the most appropriate for theoretical comparisons, because it does not appear to contain a significant amount of $1/f$ noise, and inactivation and activation components of the spectra are clearly discernable. However, other preparations may not show the latter effect. For example, the separation of the time scales of the h and m processes for squid is not as great as in the HH equations for frog node. Consequently, the separation of the two components in the theoretical spectra for squid is barely discernable (Clay, 1977).

Moore-Cox (1976) Model Spectrum

The most compelling feature of Fig. 1 is the excellent fit of Eq. (7) to the data, which immediately raises the question of whether coupled models can possibly be consistent with noise experiments. The first model of this type which will be discussed is the Moore and Cox (1976) model described by:

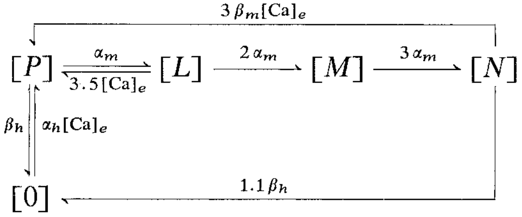

Diagram B

where $[\mathrm{Ca}]_e$ represents the relative concentration of external calcium ions and $[N]$ represents the open or conducting state. This model was designed primarily for the effects of changes of $[\mathrm{Ca}]_e$ on squid giant axon under voltage clamp observed by Frankenhaeuser and Hodgkin (1957). It also is a coupled model, since the inactivated state [0] can be attained only after activation is completed, or before it begins.

Diagram *B* has one serious drawback: namely, it does not obey microscopic reversibility. Energy is dissipated as the system moves through either one of its reaction cycles. Experiments with metabolic inhibitors would seem to indicate that this does not happen in a real axon, since the flow of ions during a nerve action potential does not require metabolic energy (Hodgkin & Keynes, 1955). However, it is possible, as Moore and Cox (1976) suggest, that the energy associated with electrical discharge of the membrane capacitance during an action potential is involved in some way.

In any case, a further drawback of their model is that it fires spontaneously, as shown by the simulation in Fig. 2. The real axon can also be made to fire spontaneously if $[\mathrm{Ca}]_e$ is lowered (Guttman & Barnhill, 1970) and this effect can be modeled satisfactorily in the HH equations by making a few simple modifications in the α's and β's (Huxley, 1957). However, both the real axon and the HH model are stable for a wide range of $[\mathrm{Ca}]_e$. Simulations of Diagram *B* with rather large increases in $[\mathrm{Ca}]_e$, or $\bar{g}_K$, or both, suggest that it does not have a region of stability. Nevertheless, noise analysis is useful in this case, because it can show the effect on the theoretical spectrum of one form of coupling.

The procedure for determining the spectrum of this model is the same as described by Eq. (3). That is, N_∞ and $N_0(t)$ must be found, which is effected by writing the equations for the model in matrix form,

$$\begin{pmatrix} \dot{L} \\ \dot{M} \\ \dot{N} \\ \dot{O} \end{pmatrix} = \begin{pmatrix} -(3\alpha_m + 3.5[\mathrm{Ca}]_e) & -\alpha_m & -\alpha_m & -\alpha_m \\ 2\alpha_m & -3\alpha_m & 0 & 0 \\ 0 & 3\alpha_m & -(3\beta_m + 1.1\beta_h) & 0 \\ -\beta_h & -\beta_h & 0.1\beta_h & -(\alpha_h[\mathrm{Ca}]_e + \beta_h) \end{pmatrix} \begin{pmatrix} L \\ M \\ N \\ O \end{pmatrix} + \begin{pmatrix} \alpha_m \\ 0 \\ 0 \\ \beta_h \end{pmatrix} \tag{8}$$

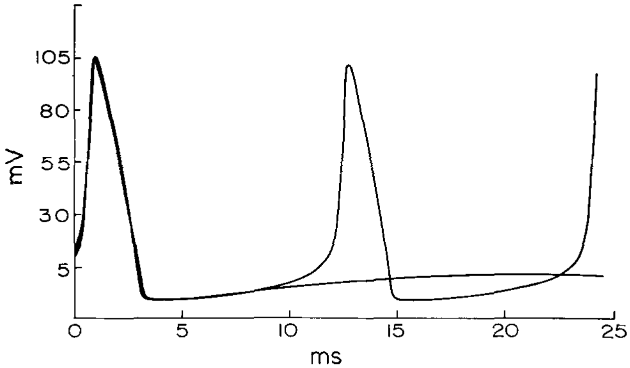

Fig. 2. Simulation of the Moore and Cox (1976) and HH models with a current shock stimulus which initially displaced the membrane potential in both to 10 mV. The time scale for the HH response has been shifted so that the action potentials can be compared. They essentially overlap, although the Moore-Cox response does not have the "gratuitous bump" which occurs during repolarization in the HH model. However, it produces a continuous train of action potentials, as shown in the figure. Moreover, it fires spontaneously, even without the initial stimulus. The HH model produces a slight oscillatory voltage overshoot, but it does not fire spontaneously for the normal conditions used in this simulation. (Runge-Kutta simulation with 1-μsec time step)

where the conservation of probability, $P+L+M+N+O=1$, has been used. Eq. (8) can be written symbolically as

$$\dot{\mathbf{q}}=\mathbf{A}\mathbf{q}+\mathbf{r} \tag{9}$$

where $\mathbf{q}$ is the vector (L, M, N, O), $\mathbf{r}=(\alpha_m, 0, 0, \beta_h)$, and $\mathbf{A}$ is the matrix of transition probabilites in Eq. (8). The solution to the latter is (Hildebrand, 1965)

$$\mathbf{q}=e^{\mathbf{A}t}\mathbf{q}(0)+\int_0^t e^{\mathbf{A}(t-s)}\mathbf{f}\,ds \tag{10}$$

where $\mathbf{q}(0)=(0, 0, 1, 0)$ is the initial condition corresponding to Eq. (3), and

$$e^{\mathbf{A}t}=\sum_1^4 e^{\lambda_k t} f_k(\mathbf{A}). \tag{11}$$

The quantities λ_k, $k=1, \ldots, 4$, are the eigenvalues of $\mathbf{A}$ and

$$f_k(\mathbf{A})=\prod_{j\neq k}^4(\mathbf{A}-\lambda_k\mathbf{I})/\prod_{j\neq k}^4(\lambda_k-\lambda_r) \tag{12}$$

where $\mathbf{I}$ is the identity matrix. Consequently, the solution for $N_0(t)$ is

$$N_0(t)=\sum_1^4 e^{\lambda_k t}\{f_k(\mathbf{A})\}_{3,3}+\sum_1^4\frac{(e^{\lambda_k t}-1)}{\lambda_k}[\alpha_m\{f_k(\mathbf{A})\}_{3,1}+\beta_h\{f_k(\mathbf{A})\}_{3,4}]. \tag{13}$$

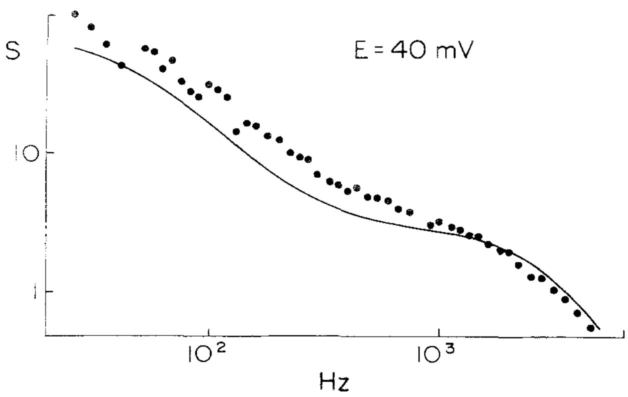

Fig. 3. Same data as Fig. 1. Solid line is $S(f)$ calculated from the Moore and Cox (1976) model with α's and β's appropriate for frog node of Ranvier

The eigenvalues λ_k are the solutions to the fourth order characteristic equation $|\mathbf{A}-\lambda\mathbf{I}|=0$, which may be determined straightforwardly on a computer.

The spectrum at 40 mV depolarization of this model as determined from the Fourier transform of Eq. (3) with the results for N_∞ and $N_0(t)$ inserted is given in Fig. 3 along with the data from Conti *et al.* (1976). The result is inconsistent with the data, but the similarity of shape to the HH model spectrum is interesting.

Jakobsson (1978) Model Spectrum

A second coupled model which does satisfy microscopic reversibility is that of Jakobsson (1978), described by

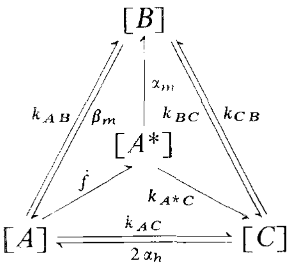

Diagram C

with conductance proportional to B^3 and

$$k_{A^*C}=k_{BC}=\beta_{h,\,E-10}/3,$$
$$k_{AB}=\beta_m m_\infty/(2-m_\infty)$$
$$k_{AC}=4\alpha_h(1-h_\infty^{1/3})/(h_\infty^{1/3}(2-m_\infty))$$
$$k_{CB}=m_\infty\beta_{h,\,E-10}h_\infty^{1/3}/(6(1-h_\infty^{1/3}))$$

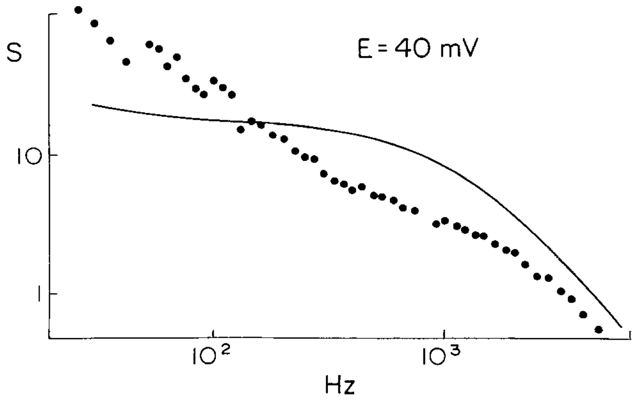

Fig. 4. Same data as Fig. 1. Solid line is $S(f)$ calculated from the Jakobsson (1978) model with α's and β's appropriate for frog node of Ranvier

where $\beta_{h,E-10}$ is the same as β_h, but with the voltage shifted by 10 mV in the hyperpolarizing direction, and $\dot{f}$ is the time derivative of a voltage-dependent function f. This model is designed primarily for the inactivation phenomena described previously. It has the novel feature of a transient state A^* which is inaccesible during steady voltage clamp. That is, A^* does not affect the calculation of theoretical spectra for the model.

Since $g_{\mathrm{Na}} \sim B^3$, the microscopic interpretation of the model consists of three statistically independent particles, any one of which can be in the open state $[B]$, or in either $[A]$ or $[C]$. The latter two states can be interpreted as being the normal resting state and the inactivated state, respectively, for each particle. That is, this model is a modification of the HH picture in which each of the three m particles not only has the normal closed state $\bar{m}$, but an additional closed state, as well, which is controlled primarily by the inactivation kinetic parameters α_h and β_h. That is, inactivation and activation are completely coupled. The kinetic diagram for this three particle system is constructed in a way which is rather similar to HH. The result is:

$$\begin{tikzcd}
{[0_B, 0_A]} \arrow[r, shift left, "3k_{CA}"] \arrow[d, shift right, "3k_{CB}"'] & {[0_B, 1_A]} \arrow[l, shift left, "k_{AC}"] \arrow[r, shift left, "2k_{CA}"] \arrow[d, shift right, "2k_{CB}"'] \arrow[dl, shift left, "k_{AB}"] & {[0_B, 2_A]} \arrow[l, shift left, "2k_{AC}"] \arrow[r, shift left, "k_{CA}"] \arrow[d, shift right, "k_{CB}"'] \arrow[dl, shift left, "2k_{AB}"] & {[0_B, 3_A]} \arrow[l, shift left, "3k_{AC}"] \arrow[dl, shift left, "3k_{AB}"] \\
{[1_B, 0_A]} \arrow[u, shift right, "k_{BC}"'] \arrow[ur, shift left, "k_{BA}"] \arrow[r, shift left, "2k_{CA}"] \arrow[d, shift right, "2k_{CB}"'] & {[1_B, 1_A]} \arrow[u, shift right, "k_{BC}"'] \arrow[ur, shift left, "k_{BA}"] \arrow[l, shift left, "k_{AC}"] \arrow[r, shift left, "k_{CA}"] \arrow[d, shift right, "k_{CB}"'] \arrow[dl, shift left, "k_{AB}"] & {[1_B, 2_A]} \arrow[u, shift right, "k_{BC}"'] \arrow[ur, shift left, "k_{BA}"] \arrow[l, shift left, "2k_{AC}"] \arrow[dl, shift left, "2k_{AB}"] & \\
{[2_B, 0_A]} \arrow[u, shift right, "2k_{BC}"'] \arrow[ur, shift left, "2k_{BA}"] \arrow[r, shift left, "k_{CA}"] \arrow[d, shift right, "k_{CB}"'] & {[2_B, 1_A]} \arrow[u, shift right, "2k_{BC}"'] \arrow[ur, shift left, "2k_{BA}"] \arrow[l, shift left, "k_{AC}"] \arrow[dl, shift left, "k_{AB}"] & & \\
{[3_B, 0_A]} \arrow[u, shift right, "3k_{BC}"'] \arrow[ur, shift left, "3k_{BA}"] & & &
\end{tikzcd}$$

Diagram D

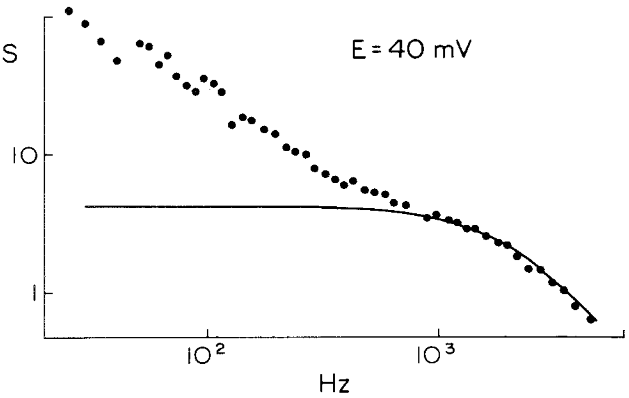

Fig. 5. Same data as Fig. 1. Solid line is $S(f)$ calculated from Diagram E with α's and β's appropriate for frog node of Ranvier

where $[m_B, n_A]$ refers to the number of particles in states B and A, respectively, and conduction occurs only in state $[3_B, 0_A]$.

The theoretical noise spectrum requires B_∞^3 and $B^3(t)$, which can be determined from Diagram C. The result, shown in Fig. 4, has a very different shape than HH or Moore-Cox, and it is clearly inconsistent with the data.

Armstrong and Bezanilla (1977) Model Spectrum

Recently Armstrong and Bezanilla (1977) have proposed a model based on gating current measurements. The model is somewhat qualitative, as not all of the rate constants are described. However, it bears some similarity to:

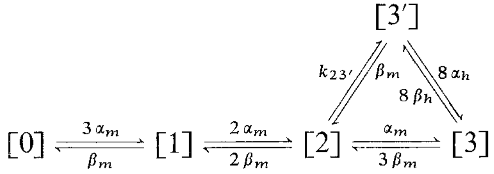

Diagram E

where $k_{23'}$ is determined from microscopic reversibility to be $\alpha_m \beta_h/(3\alpha_h)$, and conduction occurs only in state [3]. The activation portion of this scheme is identical to HH, but the inactivation process is different, since it can occur only when 2 or 3 of the m particles are open. Consequently, the conductance cannot be written in the $m^3 h$ form. It is given by the probability that the system is in state [3], which can be determined by the matrix methods employed for the Moore-Cox model. The particular choice of $8\alpha_h$ and $8\beta_h$ for the rate constants between [3] and the inactivated state [3′] is apparently supported by gating current measurements (Arm-

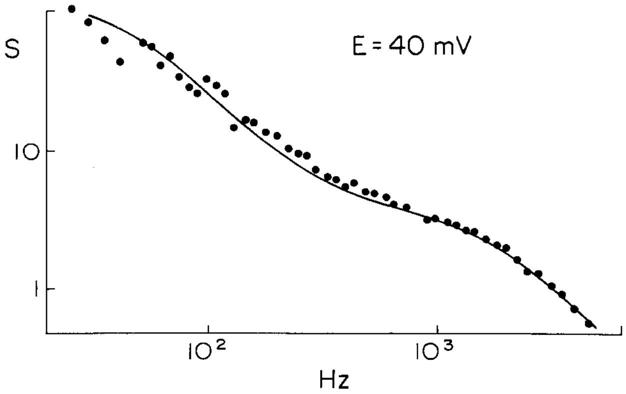

Fig. 6. Same data as Fig. 1. Solid line is $S(f)$ calculated from Diagram F

strong & Bezanilla, 1977). These authors state that the half power frequency of the inactivation component of the spectrum should be significantly different from HH because of these particular rate constants. The spectrum for Diagram *E* is certainly different than HH, as shown in Fig. 5. The half power frequency for the inactivation component cannot, in fact, be determined, since the latter is effectively obscured by the activation components. This finding is insensitive to the particular choice of rate constants connecting state [3′] to [2] and [3]. It appears to be a function of the structure of Diagram *E*.

An Alternative Coupling Scheme

The similarity of the Moore-Cox spectrum to HH suggests the related kinetic cycle:

$$\begin{tikzcd}
 & & & {[3']} \arrow[dlll, shift left, "\alpha_h"] \arrow[drrr, shift left, "\alpha_h"] & & & \\
{[0]} \arrow[urrr, shift left, "k_{03'}"] \arrow[rr, shift left, "3\alpha_m"] & & {[1]} \arrow[ll, shift left, "\beta_m"] \arrow[rr, shift left, "2\alpha_m"] & & {[2]} \arrow[ll, shift left, "2\beta_m"] \arrow[rr, shift left, "\alpha_m"] & & {[3]} \arrow[ll, shift left, "3\beta_m"] \arrow[ulll, shift left, "\beta_h"]
\end{tikzcd}$$

Diagram F

where $k_{03'} = (\alpha_m/\beta_m)^3 \beta_h$, so that microscopic reversibility is satisfied. Coupling occurs in this model, as in Moore-Cox, since the inactivated state can be attained only when all or none of the three *m* particles are open. This may be a promising mechanism, since the spectrum is rather similar to HH, as shown in Fig. 6, with the greatest deviation occurring at low frequencies. For this comparison the scatter in the data of Conti *et al.* (1976) is sufficiently great so that Diagram F cannot be immediately ruled out.

Discussion

This paper is not intended to be a thorough noise analysis of all of the models which have been proposed for Na conductance in nerve. However, it is a fair sample of the different classes of theoretical coupling mechanisms. One obvious modification of the various diagrams which was not analyzed is to allow conduction in more than one state. The voltage dependence of the noise amplitude is affected by such a change, but the shape of $S(f)$ is not significantly altered, if the relative conductance of the additional open states is small (Chen & Hill, 1973). Conti *et al.* (1976) find that the single conducting state HH model (Diagram *A*) adequately accounts for the voltage dependence of their data, although the aggrement is not significantly altered if state [2] conducts at the 0.01 level relative to state [3]. If this figure were substantially higher, both the noise data and the macroscopic conductance would be significantly altered. For example, if the relative conductance of state [2] were κ, $g_{\mathrm{Na}} \sim m^3 h$ would be replaced by $g_{\mathrm{Na}} \sim m^3 h + 3\kappa m^2(1-m)h$. If $\kappa \sim 1$, it would seem that standard voltage clamp analysis might detect this second conducting state.

The comparison between the theoretical spectra and the noise data would appear to rule out all but HH and the model in Diagram *F*. A second point in favor of the latter is that it appears to be consistent with the inactivation delay experiment (Bezanilla & Armstrong, 1977) which cannot be explained by HH. However, any model must be subjected to the complete list of experimental tests. The point of this paper is simply to add noise analysis to that list.

Clearly, more noise data is needed from other preparations and from frog node at larger depolarizing voltages than 40 mV. Unfortunately, reliable stationary noise records are difficult to obtain over a large range of voltages, because of inactivation. Sigworth (1977) has recently shown that noise information can be obtained at large depolarizations using nonstationary noise analysis. His data offer further support for the idea that conduction occurs only in one state. However, the detailed model testing proposed in this study probably requires frequency analysis, which can be reliably performed only on stationary noise records.

The author gratefully acknowledges useful discussions during the early phase of this work with Louis DeFelice and Eric Jakobsson.

This work was supported by a grant from the National Institutes of Health: HL05346-01A1.

References

Armstrong, C.M., Bezanilla, F. 1977. Inactivation of the sodium channel. II. Gating current experiments. *J. Gen. Physiol.* **70**:567

Bezanilla, F., Armstrong, C.M. 1975. Properties of the sodium channel gating current. *Cold Spring Harbor Symp. Quant. Biol.* **40**:297

Bezanilla, F., Armstrong, C.M. 1977. Inactivation of the sodium channel. I. Sodium Current Experiments. *J. Gen. Physiol.* **70**:549

Chen, Y.D., Hill, T.L. 1973. Fluctuations and noise in kinetic systems. Application to K^+ channels in the squid axon. *Biophys. J.* **13**:1276

Chiu, S.Y. 1976. Observations on sodium channel inactivation in frog nerve. *Biophys. J.* **16**:25*a (Abstr.)*

Clay, J.R. 1977. A comparison of ion current noise predicted from different kinetic models of the sodium channel. *Biophys. J.* **17**:12*a (Abstr.)*

Connor, J.A. 1976. Sodium current inactivation in crustacean axons. *Biophys. J.* **16**:24*a (Abstr.)*

Conti, F., DeFelice, L.J., Wanke, E. 1975. Potassium and sodium ion current noise in the membrane of the squid giant axon. *J. Physiol. (London)* **248**:45

Conti, F., Hille, B., Neumcke, B., Nonner, W., Stämpfli, R. 1976. Measurement of the conductance of the sodium channel from current fluctuations at the node of Ranvier. *J. Physiol. (London)* **262**:699

Fitzhugh, R. 1965. A kinetic model of the conductance changes in nerve membrane. *J. Cell. Comp. Physiol.* **66**:111

Frankenhaeuser, B., Hodgkin, A.L. 1957. The action of calcium on the electrical properties of squid axons. *J. Physiol. (London)* **137**:218

Goldman, L., Schauf, C.L. 1973. Quantitative description of sodium and potassium currents and computed action potentials in *Myxicola* giant axons. *J. Gen. Physiol.* **61**:361

Guttman, R., Barnhill, R. 1970. Oscillation and repetitive firing in squid axons. Comparison of experiments with computations. *J. Gen. Physiol.* **55**:104

Hildebrand, F.B. 1965. Methods of Applied Mathematics. Prentice Hall, Englewood Cliffs

Hill, T.L., Chen, Y.D. 1972. On the theory of ion transport across the nerve membrane. IV. Noise from the open-close kinetics of K channels. *Biophys. J.* **12**:948

Hodgkin, A.L., Huxley, A.F. 1952. A quantitative description of membrane current and its application to conduction and excitation in nerve. *J. Physiol. (London)* **117**:500

Hodgkin, A.L., Keynes, R.D. 1955. Active transport of cations in giant axons from *Sepia* and *Loligo*. *J. Physiol. (London)* **128**:28

Huxley, A.F. 1957. Ion movements during nerve activity. *Ann. N.Y. Acad. Sci.* **81**:221

Jakobsson, E. 1978. A fully coupled transient excited state model for the sodium channel. I. Conductance in the voltage clamped case. *J. Math. Biol. (in press)*

Moore, J.W., Cox, E.B. 1976. A kinetic model for the sodium conductance in squid axon. *Biophys. J.* **16**:171

Neher, E., Sakmann, B. 1976. Single channel currents recorded from membrane of denervated frog muscle fibres. *Nature (London)* **260**:799

Neher, E., Stevens, C.F. 1977. Conductance fluctuations and ionic pores in membranes. *Annu. Rev. Biophys. Bioeng.* **6**:345

Oxford, G.S., Pooler, J.P. 1975. Selective modification of sodium channel gating in lobster axons by 2,4,6, trinitrophenol. Evidence for two inactivation mechanism. *J. Gen. Physiol.* **66**:765

Peganov, E.M. 1973. Kinetics of sodium channel inactivation in the frog Ranvier node. *Bull. Exp. Biol. Med.* **76**:1254

Sigworth, F.J. 1977. Sodium channels in nerve apparently have two conducting states. *Nature (London)* **270**:265

Stevens, C.F. 1972. Inferences about membrane properties from electrical noise measurements. *Biophys. J.* **12**:1028

Wang, M.C., Uhlenbeck, G.E. 1954. On the theory of Brownian motion. *In:* Selected Papers on Noise and Stochastic Processes. N. Wax, editor. Dover, New York